ELSEVIER
www.elsevier.com/locate/jsaerev

JSAE Review 24 (2003) 449–456

Independent wheel torque control of small-scale electric vehicle for handling and stability improvement

Motoki Shino[a], Masao Nagai[b]

[a] *Department of Engineering Synthesis, The University of Tokyo, 7-3-1 Hongo, Bunkyo-ku, Tokyo, 113-8656, Japan*
[b] *Department of Mechanical Systems Engineering, Tokyo University of Agriculture and Technology, Koganei-shi, Tokyo, 184-8588, Japan*

Received 4 March 2003; received in revised form 21 April 2003

Abstract

This paper examines the feasibility of the proposed control in a small-scale electric vehicle with two independent motors equipped at the rear axles. The direct yaw moment control system is designed with the application of model matching control theory. For realizing the proposed system in an actual electric vehicle, it is necessary to estimate the side slip angle instead of measuring it directly. A speed-dependent observer is proposed in this paper. Experiments using actual small-scale electric vehicle are carried out to verify the effectiveness of the proposed chassis control system on lateral stability in a J-turn test and lane change tests.

1. Introduction

Nowadays, because of the current air pollution problems from automobiles in large cities, it is expected that low emission vehicles such as electric vehicles or hybrid electric vehicles will become popular. This paper focuses on designing a controller for a small-scale electric vehicle to enhance active safety in critical driving situations [1]. Based on such considerations, some stability control systems have been developed and commercially used [2–4]. However, it is not theoretically clear how the control system of the electric vehicle can be optimally designed to improve the handling and stability against arbitrary steer input and in critical driving situations.

fAt the beginning of our research, the electric vehicle, as a representative of clean-energy vehicles of this century, was used as a research object for improving handling and stability of vehicle [5]. Compared with the conventional passenger cars powered by the gasoline engine, the better response of electric vehicles powered by an electric motor can generate traction or braking forces more precisely [6,7]. Moreover, commonly, electric vehicles are equipped with in-wheel-motors which can control the traction and braking forces independently. Based on these structural merits, vehicle motion can be stabilized by yaw moment generated as a result of the difference in tire traction or braking forces between the right and left side of the vehicle, which is so-called "Direct Yaw-moment Control" (DYC).

This paper proposes a chassis control system utilizing DYC by using the model matching control method to make the steering response of the body side slip angle constantly zero. With the goal of enhancing stability, the control objective is to obtain desirable steering response by controlling the body side slip angle of the vehicle. Experiments using actual small-scale electric vehicle are carried out to verify the effectiveness of the proposed chassis control system on cornering performance.

2. Description of small-scale electric vehicle "novel

An electric vehicle named "NOVEL", as shown in Fig. 1, is a one person rear-wheel drive vehicle with two-kW DC-brushless-motors equipped at each of the rear wheels. Such structure is so-called "in-wheel-motor" structure. The vehicle is 400 kg in weight (driver included), has 50 km/h maximum speed, and good acceleration performance, as it takes 10 s to accelerate the vehicle from 0 to 40 km/h. This vehicle can detect the input maneuvers of the driver and motion states of the vehicle on-line and can control the driving torques of rear wheels independently by the in-wheel-motor structure. The measured input maneuvers from the driver are acceleration pedal stroke and steering wheel angle. The

0389-4304/$30.00
doi:10.1016/S0389-4304(03)00080-8

JSAE20034531

Fig. 1. Small-scale electric vehicle "NOVEL".

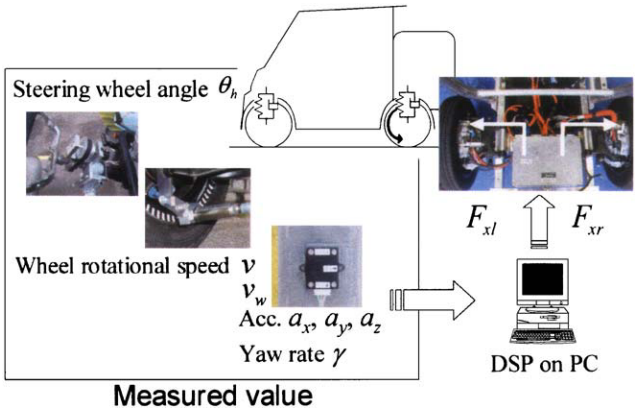

Fig. 2. Description of experiment vehicle "NOVEL".

measured motion states of the vehicle are lateral, longitudinal, vertical accelerations, yaw rate, roll rate at the center of gravity, and each tire wheel velocity. All measured values of both the input maneuvers and the motion states of the vehicle are input into digital signal processing (DSP) in real-time. Then, the command torque for each in-wheel-motor is calculated as the output of the control system.

For a direct yaw-moment stabilization system, it is necessary to sense the steering wheel angle input from driver, the yaw rate at the center of gravity, the driving wheel velocity, and the vehicle body velocity as shown in Fig. 2. The steering wheel angle is measured by the application of a rotary position coder. The yaw rate is measured by a gyro sensor. The driving wheel velocity is measured directly by a rotary encoder, while the vehicle body velocity is measured indirectly from the non-driving wheel velocity (front wheel) by the rotary encoder. These measurement values are used to calculate the command torques for the direct yaw-moment control system, which will be explained in section 3. The command torques are then input to each in-wheel-motor of the rear axle.

3. Direct yaw-moment control system design

3.1. Control objective

In order to improve the handling and stability of the vehicle, the side slip angle and yaw rate of the vehicle are controlled to desired values using the direct yaw-moment system. The direct yaw-moment generated by the traction force at the rear axle is employed as the control input to make actual response trace the desired values. With the application of model matching control technique, the control system consists of a feedforward compensator for to the steering angle, and a feedback compensator depending on state deviations of side slip angle and yaw rate.

3.2. Identification of vehicle model for controller design

This paper proposes a chassis control system using linear control theory to control the actual vehicle which commonly has nonlinear characteristics. Hence, it is necessary to know the cornering characteristics of NOVEL with respect to steering angle input before the controller design is conducted. This section describes the identification of an equivalent two-wheel model of the vehicle in planar motion to avoid complexity in the controller design as shown in Fig. 3. The vehicle model has two degrees-of-freedom, i.e., the yaw, and the lateral motions. The coordinate system is fixed on the vehicle when setting up the equations of motions. The characteristics of the tire is assumed to be a linear model where the lateral force is proportional to the tire side slip angle, in the case of the side slip angle being small. Under these assumptions, the governing

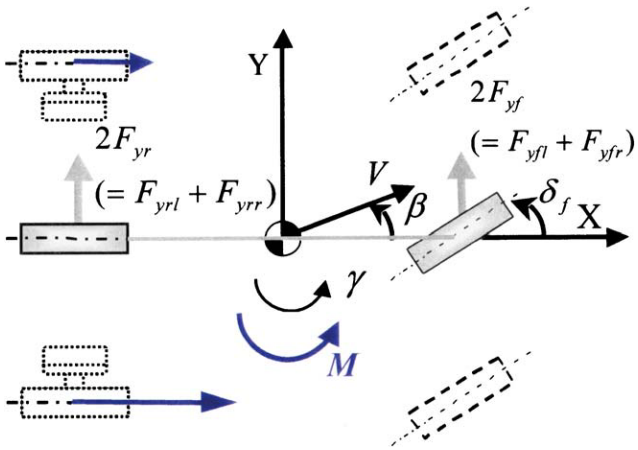

Fig. 3. Vehicle model for controller design.

equations of the lateral and yaw motions of the vehicle can be expressed as follows:

Lateral motion:

$$mV(\dot{\beta}+\gamma) = -2C_f(\beta+\gamma l_f/V-\delta_f) - 2C_r(\beta-\gamma l_r/V), \quad (1)$$

Yaw motion:

$$I_z\dot{\gamma} = -2C_f l_f(\beta+\gamma l_f/V-\delta_f)+2C_r l_r(\beta-\gamma l_r/V), \quad (2)$$

where m denotes the mass of the body, β the side slip angle, γ the yaw rate, l_f and l_r the distances from the center of gravity (CG) to the front and rear axles, respectively, V the chassis velocity, I_z the yaw moment of inertia. C_f and C_r the equivalent front and rear cornering stiffness, respectively, and δ_f the front steering angle input from driver.

From the above equations, the equivalent two-wheel model needs the following parameters: m, I_z, l_f, l_r, C_f, C_r. In their parameters, the tire cornering stiffness, C_f, C_r are very difficult to measure directly because their values include the dynamics characteristics of suspension, tire etc. In this paper, based on an experiment on a small-scale electric vehicle and simulation from an analytical model, the cornering stiffnesses is determined by trial and error. When the same steering maneuver is input in both the experiment and the simulation at a constant velocity of 35 km/h, the output of the yaw rate is shown in Figs. 4 and 5. Fig. 4 shows the time response of the yaw rate when executing a J-turn maneuver on a dry asphalt road. Fig. 5 shows the frequency response of the yaw rate with respect to the front steering input. As a result, as compared with the experiment and the simulation, the identification result is quite satisfactory. The measured and identified parameters of NOVEL are shown in Table 1. In addition, from static analysis of steering characteristics, it is apparent that NOVEL has weak understeer characteristics.

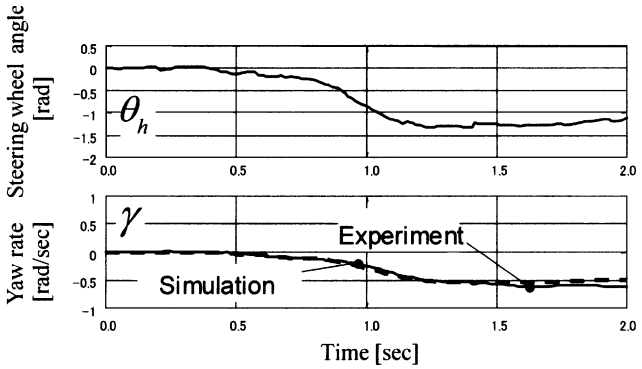

Fig. 4. Identification result of yaw rate response ($V=35$ km/h).

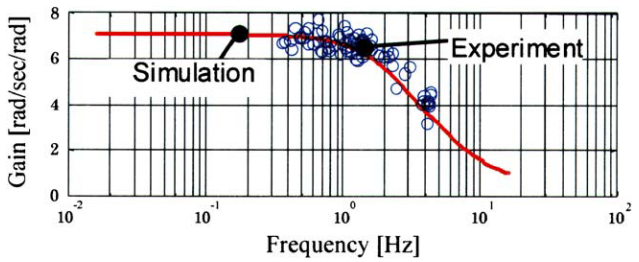

Fig. 5. Frequency response obtained from identification ($V=35$ km/h).

Table 1
Parameters of experiment vehicle "NOVEL"

Definition	Symbol	Unit	Value
Vehicle mass (including driver)	m	kg	400
Yaw moment of inertia	I_z	Kgm^2	160
Wheel base	l	m	1.28
Axle tread	d	m	0.82
Distance from CG to front axle	l_f	m	0.75
Distance from CG to rear axle	l_r	m	0.53
Height of CG	h	m	0.4
Front cornering stiffness	C_f	N/rad	10,000
Rear cornering stiffness	C_r	N/rad	16,000
Steer gear ratio	n	–	18.7

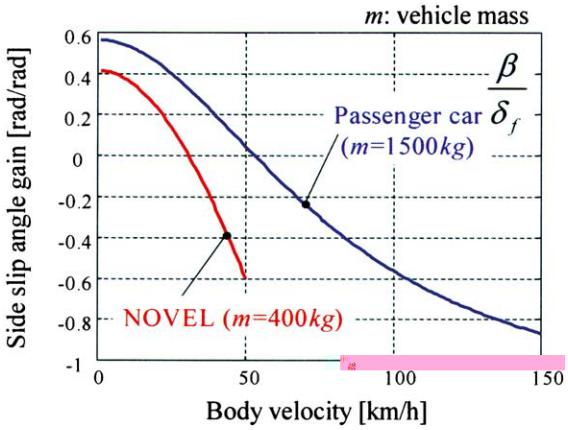

Fig. 6. Side slip angle characteristics with respect to chassis velocity at steady state cornering.

Using an analytical model, Fig. 6 shows the body side slip angle of NOVEL, compared with a normal passenger car. Although NOVEL has a maximum speed of 50 km/h, its body side slip angle during steady state cornering is in the same level as the high speed region of the passenger car. Therefore, in order to enhance safety, it is necessary to control the body side slip angle of such small-scale electric vehicles.

3.3. Yaw-moment controller design

To make the side slip angle and yaw rate follow the desired value with respect to the steering input this paper applies the model matching theory to design the system. This is based on the fact that it is very difficult for the driver to control the side slip angle and it is reported that most traffic accidents occur due to

excessive side slip of vehicles [8]. Therefore, it is important to suppress the body side slip angle.

First, from Eqs. (1) and (2), the state equation of the vehicle model for designing the controller can be obtained as follows:

$$\begin{bmatrix}\dot\beta\\ \dot\gamma\end{bmatrix}=\begin{bmatrix}a_{11} & a_{12}\\ a_{21} & a_{22}\end{bmatrix}\begin{bmatrix}\beta\\ \gamma\end{bmatrix}+\begin{bmatrix}b_1\\ b_2\end{bmatrix}M+\begin{bmatrix}h_1\\ h_2\end{bmatrix}\delta_{\mathrm{f}},$$

$$\dot X = AX + BM + H\delta_{\mathrm{f}}, \tag{3}$$

where

$$X=\begin{bmatrix}\beta\\ \gamma\end{bmatrix},\quad \begin{bmatrix}b_1\\ b_2\end{bmatrix}=\begin{bmatrix}0\\ \dfrac{1}{I_z}\end{bmatrix},\quad \begin{bmatrix}h_1\\ h_2\end{bmatrix}=\begin{bmatrix}\dfrac{2C_{\mathrm{f}}}{mV}\\ \dfrac{2C_{\mathrm{f}}l_{\mathrm{f}}}{I_z}\end{bmatrix},$$

$$\begin{bmatrix}a_{11} & a_{12}\\ a_{21} & a_{22}\end{bmatrix}=\begin{bmatrix}\dfrac{-2(C_{\mathrm{f}}+C_{\mathrm{r}})}{mV} & \dfrac{-2(C_{\mathrm{f}}l_{\mathrm{f}}-C_{\mathrm{r}}l_{\mathrm{r}})}{mV^2}-1\\ \dfrac{-2(C_{\mathrm{f}}l_{\mathrm{f}}-C_{\mathrm{r}}l_{\mathrm{r}})}{I_z} & \dfrac{-2(C_{\mathrm{f}}l_{\mathrm{f}}^2+C_{\mathrm{r}}l_{\mathrm{r}}^2)}{I_zV}\end{bmatrix}.$$

Moreover, the transfer function are derived as follows:

$$\beta(s)=\frac{(h_1s-h_1a_{22}+h_2a_{12})\delta_f(s)+b_2a_{12}M(s)}{(s-a_{11})(s-a_{22})-a_{21}a_{12}}, \tag{4}$$

$$\gamma(s)=\frac{(h_2s+h_1a_{21}-h_2a_{11})\delta_f(s)+b_2(s-a_{11})M(s)}{(s-a_{11})(s-a_{22})-a_{12}a_{21}}. \tag{5}$$

The feedforward compensation is designed to regulate the side slip angle in steady state to cornering zero. For that purpose, the relationship between the control input M_{ff} and the front steering angle δ_{f} is assumed to be as follows:

$$M_{\mathrm{ff}} = G_{\mathrm{ff}}\delta_{\mathrm{f}}, \tag{6}$$

where G_{ff} is the proportional gain of feedforward controller. By substituting the above equation into Eq. (4), the side slip angle equation in steady state cornering condition can be obtained as follows:

$$\frac{\beta_0}{\delta_{\mathrm{f}0}}=\frac{-h_1a_{22}+h_2a_{12}+b_2a_{12}G_{\mathrm{ff}}}{a_{11}a_{22}-a_{21}a_{12}}. \tag{7}$$

In order to obtain zero value of side slip angle β_0, the numerator of the above equation must equal zero. Acoordingly, the feedforwad gain G_{ff} can be obtained as follows:

$$G_{\mathrm{ff}}=\frac{h_1a_{22}-a_{12}h_2}{a_{12}b_2}. \tag{8}$$

As a result, the transfer function from the front steering angle to the yaw rate can be written by substituting Eqs. (6) and (8) into Eq. (5):

$$\frac{\gamma(s)}{\delta_{\mathrm{f}}(s)}=\frac{h_1a_{22}s+h_1(a_{12}a_{21}-a_{11}a_{22})}{a_{12}\{s^2+(-a_{11}-a_{22})s+(a_{11}a_{22}-a_{12}a_{21})\}}. \tag{9}$$

Moreover, the desired model is determined such that the side slip angle response $\beta_d(s)$ is constantly zero, and the yaw rate response $\gamma_d(s)$ is set to be the first order lag with respect to the front steering angle as follows:

$$\dot X_d = A_dX_d + H_d\delta_{\mathrm{f}}, \tag{10}$$

where

$$X_d=\begin{bmatrix}\beta_d\\ \gamma_d\end{bmatrix},\quad X_d=\begin{bmatrix}\beta_d\\ \gamma_d\end{bmatrix},\quad H_d=\begin{bmatrix}0\\ \dfrac{k_{\gamma d}}{\tau_{\gamma d}}\end{bmatrix}.$$

$k_{\gamma d}$ and $\tau_{\gamma d}$ are steady state gain and time constant of yaw rate response, respectively. Moreover, it is important to consider what is an ideal response of the desired model in this controller. Then, the transfer function of the desired yaw rate shown in Eq. (9) with the transfer function shown in Eq. (10) are compared. By conducting design such that the two yaw rates converge to the same value in the steady state and high frequency region, the following values can be obtained:

$$k_{\gamma d}(V)=\frac{h_1}{a_{12}},\quad \tau_{\gamma d}=\frac{a_{12}}{h_1a_{22}}k_{\gamma d}(V). \tag{11}$$

Generally, there is limitation in using only feedforward compensation to control the vehicle, especially when the vehicle runs against external disturbance (i.e. crosswind, etc.) or runs into some unexpected changes (i.e. road surface condition, etc.). Therefore, it is necessary to additionally provide a feedback compensator against such disturbance and modeling error. Therefore, a feedback compensator is coupled with feedforward compensation to obtain the desired performance. First, the state deviation between the desired value X_d and actual value X is assumed to be as follows:

$$E = X - X_d. \tag{12}$$

The differentiated value of the above equation can be obtained as follows:

$$\begin{aligned}\dot E &= \dot X - \dot X_d\\ &= A(X-X_d)+BM_{\mathrm{fb}}+(A-A_d)X_d+(H-H_d)\delta_{\mathrm{f}}\\ &= AE+BM_{\mathrm{fb}}+(A-A_d)X_d+(H-H_d)\delta_{\mathrm{f}}.\end{aligned} \tag{13}$$

If the third and fourth terms in this equation are considered to be the disturbance, W which depends on the front steering angle is as follows:

$$\dot E = AE + BM_{\mathrm{fb}} + W. \tag{14}$$

If the disturbance terms are taken as zero, the optimal control input can be calculated by state feedback of deviations of the side slip angle and yaw rate as follows:

$$\begin{aligned}M_{\mathrm{fb}} &= -G_{\mathrm{fb}}E\\ &= -g_{\mathrm{fb}1}(\beta-\beta_d)-g_{\mathrm{fb}2}(\gamma-\gamma_d),\end{aligned} \tag{15}$$

where the feedback gains g_{fb1}, g_{fb2} are determined to minimize the following performance index:

$$J=\int_0^\infty\left(\left(\frac{\beta-\beta_d}{q_{\mathrm{fb}1}}\right)^2+\left(\frac{\gamma-\gamma_d}{q_{\mathrm{fb}2}}\right)^2+\left(\frac{M_{\mathrm{fb}}}{r_{\mathrm{fb}}}\right)^2\right)\mathrm{d}t, \tag{16}$$

Table 2
Weight value of feedback controller

Side slip angle (rad)	Yaw rate (rad/s)	Yaw moment (Nm)
q_{fb1}	q_{fb2}	r_{fb}
1×10^{-3}	1×10^{-2}	2×10^{2}

where the weighting coefficients q_{fb1}, q_{fb2} indicate the maximum allowable values of the state variables and the coefficients r_{fb} indicates the limit of control input as shown in Table 2.

3.4. Distribution of driving force

In the previous section, the direct yaw-moment was determined to improve the handling and cornering of the vehicle. This section proposes a distribution of traction force to generate the yaw-moment. The small-scale electric vehicle is equipped with in-wheel-motors which can control the traction forces independently. Moreover, each traction force can be realized by using the motor with a built-in torque feedback controller.

When the longitudinal acceleration of the vehicle is a_x, the governing equation of longitudinal motion can be expressed as follows:

$$ma_x = F_{xl} + F_{xr}. \tag{17}$$

Here, the yaw-moment M generated from traction forces at rear axle can be expressed as follows:

$$M = \frac{d}{2}(-F_{xl} + F_{xr}). \tag{18}$$

From Eqs. (17) and (18), in order to generate the yaw-moment in the case of acceleration a_x, the traction force of each tire can be derived respectively as follows:

$$\begin{aligned} &\textit{Left side}: \ F_{xl} = \frac{ma_x}{2} - \frac{M}{d}, \\ &\textit{Right side}: \ F_{xr} = \frac{ma_x}{2} + \frac{M}{d}. \end{aligned} \tag{19}$$

3.5. Design of speed-dependent side slip angle observer

For realizing the proposed direct yaw-moment system in the actual electric vehicle NOVEL, it is necessary to estimate the side slip angle instead of measuring it directly, since a side slip angle sensor is expensive and cannot be installed in the vehicle. According to the observer theory, the side slip angle can be estimated by measuring the steering wheel angle, the yaw rate, and the chassis velocity. As the body side slip angle has speed-dependent characteristic, it is necessary to design the side slip angle observer with variable gain depending on chassis velocity.

When the state variables of the observer are assumed to be $\hat{X} = [\hat{\beta} \quad \hat{\gamma}]^{\mathrm{T}}$, the state equation of the observer

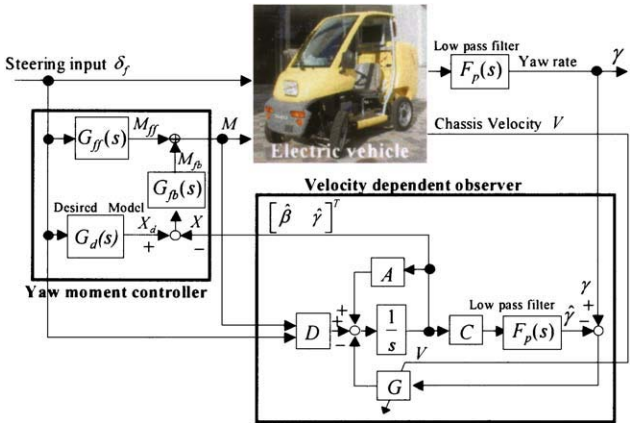

Fig. 7. Block diagram of yaw-moment-control system.

can be expressed as follows:

$$\dot{\hat{X}} = F\hat{X} + GY + DU. \tag{20}$$

The observer is designed in such a way that the error between the actual state variables and their estimated values must be zero. Thus, the state error variables can be obtained from the following equation, based on Eqs. (3) and (20):

$$\begin{aligned} \dot{e}_{ob} &= (A - GC)X - F\hat{X} + (B - D)U \\ &= (A - GC)e_{ob}. \end{aligned} \tag{21}$$

Here, the observer gains G are determined in such a way that the eigenvalues of matrix F exist in the left side of vehicle planer motion without the imaginary part in their values. Then, when the eigenvalues of A-GC are assumed to be λ_1, λ_2, the observer gains are obtained as follows:

$$\begin{aligned} G &= \begin{bmatrix} G_1(V) \\ G_2(V) \end{bmatrix} \\ &= \begin{bmatrix} -\{a_{11}(-a_{11} + \lambda_1 + \lambda_2) - \lambda_1\lambda_2 - a_{21}a_{12}\}/a_{21} \\ a_{11} + a_{22} - (\lambda_1 + \lambda_2) \end{bmatrix}. \end{aligned} \tag{22}$$

It can be seen from the above equations that the observer gains include the speed-dependent coefficients a_{11}, a_{12}, a_{21}, a_{22}. Thus the observer gains are also speed-dependent. This observer is also built-in to the low-pass filter to decrease the influence of sensor noise. Finally, the direct yaw-moment system, as shown in Fig. 7, consists of the yaw-moment controller and speed-dependent side slip angle observer.

4. Experiment studies

This section will discuss the validity of the proposed direct yaw-moment control system and the speed-dependent observer as described in Section 3 by

experiments on the small-scale electric vehicle NOVEL. The vehicle parameters are shows in Table 1.

All experiments are conducted under the condition that the road is made of dry asphalt. The air pressure of each tire is set as 150 kPa on the front wheel, and 175 kPa on the rear wheel before the experiment starts. Moreover, the front steering angle is calculated from the measured steering wheel angle divided by the overall steering gear ratio, while ignoring the steering dynamics.

4.1. Effect of speed-dependent observer

As mentioned above, it is necessary to estimate the side slip angle instead of measuring it directly. The side slip angle is estimated by measuring the chassis velocity V, the steering wheel angle θ_h, and the yaw rate γ. Fig. 8 shows the experiment results with respect to the given front steering angle and the pedal operation from the driver. Moreover, this study verifies the proposed observer by comparison with the actual yaw rate, and the estimated yaw rate because the real side slip angle is difficult to measure. Here, it is taken that the body side slip angle is correctly assumed when the estimated yaw rate matches the measured yaw rate. As a result, Fig. 8 shows that the estimated yaw rate can effectively trace the actual one by the use of the proposed observer against the changes of both velocity and steering angle. Based on repeating the experiment several times, it was confirmed that the proposed observer is effective against any arbitrary steering inputs.

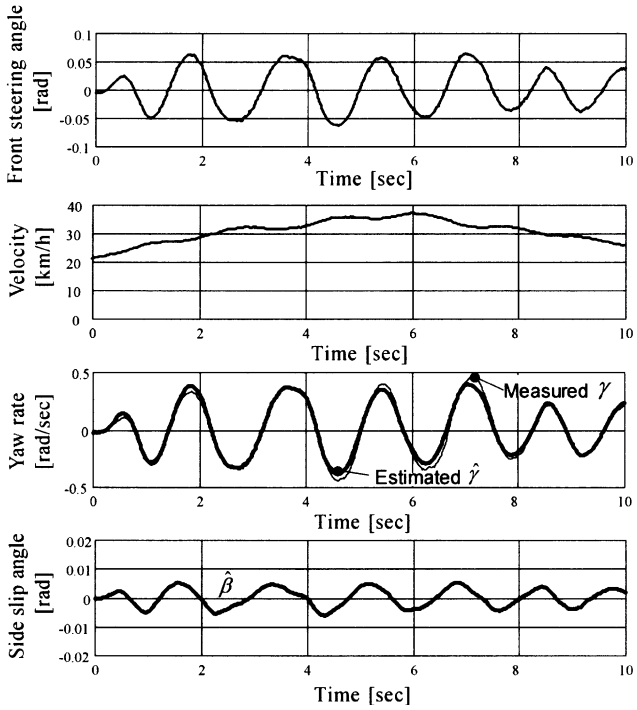

Fig. 8. Validity of speed-dependent observer.

In the next section, the validity of the yaw-moment controller using the speed-dependent side slip angle observer will be investigated.

4.2. Effect of yaw-moment controller

This section investigates the effectiveness of the proposed yaw-moment control on cornering performance. The response of the open loop system of the vehicle without consideration of the driver's operation characteristics was investigated under two conditions, when considering the disturbance term depending on the front steering angle. The J-turn and lane change tests were conducted, respectively.

4.2.1. Control effect in j-turn test

In the J-turn test shown in Fig. 9, after the vehicle runs straight at a constant speed of 35 km/h, the front steering angle pattern as shown in the upper graph of Fig. 10 is executed by the driver and input to the vehicle. This test is used to investigate vehicle behavior for steering maneuvers in the transient and steady states. Fig. 10 shows the experiment results with respect to the given steering maneuver input. Fig. 10 shows that the yaw rate response of the controlled vehicle is similar to the response without control, as the vehicle still runs on the same course. Whereas, the side slip angle response is reduced significantly by only the feedforward controller in the steady state as compared with the response of the uncontrolled vehicle. In the case of using feedforward and feedback controllers, the peak value of the side slip angle is suppressed more in the transient steering maneuver. Moreover, the yaw-moment as the control input is realized by controlling each wheel driving torque in real time as shown in the lower graph of Fig. 10. As a result, the side slip angle can be suppressed by the yaw moment control due to individual wheel torque.

4.2.2. Control effect during lane change and double lane change

In the lane change test shown in Fig. 11, after the vehicle runs straight at a constant speed of 35 km/h, the front steering angle pattern, as shown in the upper graph

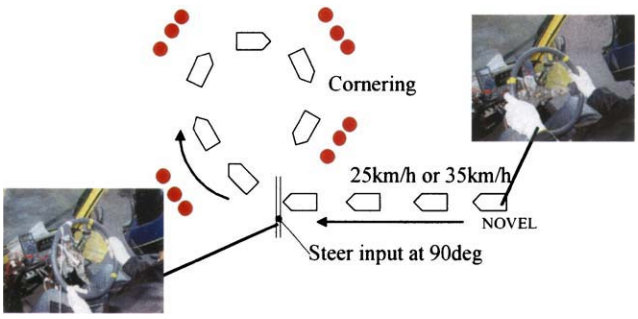

Fig. 9. Description of J-turn test.

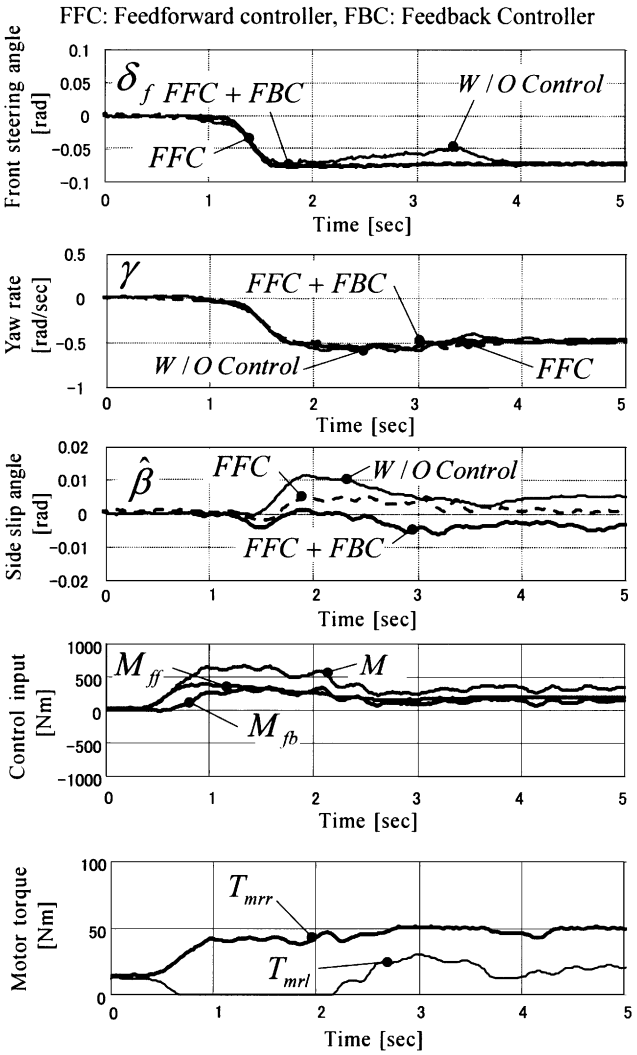

Fig. 10. Effect of yaw-moment control in J-turn ($V = 35$ km/h).

of Fig. 11, is executed by the driver. This situation can be considered as equivalent to emergency obstacle avoidance. Fig. 11 shows the experiment results of the vehicle behavior with respect to the given continuous steering maneuver input.

Fig. 11 shows that, by using only feedforward controller, the actual vehicle side slip angle can be suppressed as it becomes closer to zero as compared with the uncontrolled vehicle. It is also confirmed that firther suppression of the side slip angle can be made by the combination of feedforward and feedback controllers. Moreover, in the case without control, large body side slip angle is generated during the lane change maneuver, which causes difficulty in tracing the given trajectory. Collisions with pylons sometimes occurred. With regard to the subjective evaluation of the driver, the yaw-moment controller significantly enhances cornering stability, and handling performance so that the driver can steer the vehicle much more easily.

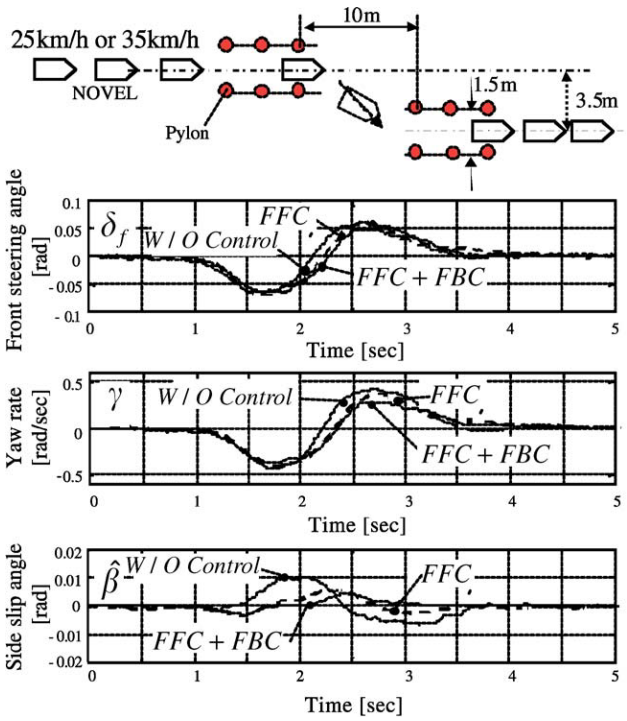

Fig. 11. Effect of yaw-moment control during lane change ($V = 35$ km/h).

5. Conclusions

Based on the concept of "drive by wire" strategy, this paper investigates the effectiveness of the proposed direct yaw-moment system that utilizes the structure merits of a small-scale electric vehicle. Experimental study using the small-scale electric vehicle NOVEL clarified the following points:

1. The small-scale electric vehicle NOVEL was developed to be able to generate the additional yaw moment by individual wheel torque command to each in-wheel-motor of the rear axle.
2. The speed-dependent observer for the side slip angle estimation proved to be feasible, based on running tests of the small-scale electric vehicle NOVEL.
3. The direct yaw-moment control system, including feedforward and feedback compensators, enhances the handling and stability during J-turn and lane change tests.

References

[1] K. Sakai, et al., Improvement in control performance of driver-vehicle system with EPS using cables to connect the steering wheel and gearbox, Proceedings of AVEC 2002, Hiroshima, Japan, 2002, pp. 641–646.
[2] M. Abe, On advanced chassis control technology for vehicle handling and active safety, Proceedings of AVEC 1996, Aachen, Germany, 1996, pp. 1–12.

[3] M. Nagai, et al., Integrated control law of active rear wheel steering and direct yaw moment control, Proceedings of AVEC 1996, Aachen, Germany, 1996, pp. 451–470.
[4] Y. Hattori, et al., Force and moment control with nonlinear optimum distribution for vehicle dynamics, Proceedings of AVEC 2002, Hiroshima, Japan, 2002, pp. 595–600.
[5] M. Shino, et al., Yaw-moment control of electric vehicle for improving handling and stability, JSAE Rev. 22 (2001) 473–480.
[6] S. Sakai, et al., Lateral motion stabilization with feedback controlled wheels, Proceedings of AVEC 2002, Hiroshima, Japan, 2002, pp. 815–820.
[7] N. Miyamoto, et al., Robust traction control of electric vehicle considering vehicle stability, Proceedings of Translog'99, Kawasaki, Japan, 1999, pp. 231–234 (in Japanese).
[8] H. Inoue, et al., Development of vehicle stability control system for active safety, J. JSAE 49 (1995) 45–51 (in Japanese with English abstract).